Uluslararası Mühendislik Araştırma ve Geliştirme Dergisi
International Journal of Engineering Research and Development
UMAGD, (2023) 15(1), 125-138.
10.29137/umagd.1147466
Cilt/Volume:15 Sayı/Issue:1 Ocak/January 2023
Araştırma Makalesi / Research Article

Robust Output Feedback Control Design for Nonlinear Coupled-tank System using Linear Matrix Inequalities

Jaffar Seyyedesmaeili[1*], **Abdullah Başçi** [1]

[1]*Electrical Engineering Department, Atatürk University, Erzurum, TÜRKİYE*

***Başvuru/Received**: 23/07/2022* ***Kabul / Accepted**: 28/11/2022* ***Çevrimiçi Basım / Published Online:** 31/01/2023*
***Son Versiyon/Final Version**: 31/01/2023*

Abstract
In this study, the Robust Output Feedback controller (ROF) is designed based on the H_∞ theory and implemented in the liquid level control of the coupled tank system. As many chemical processes have complicated and nonlinear characteristics, this robust methodology is proposed to overcome them. Hence, the vertical coupled tank system is selected as one of the popular case study systems to simulate the large scaled chemical processes to illustrate the effectiveness of the proposed ROF controller. Linear Matrix Inequalities (LMIs) methodology is selected as the main mathematical method of the design procedure. To demonstrate the performance and robustness of the ROF controller, the simulation and experimental results are compared with the Feedforward Proportional Integrator, one of the most common controllers in the industries. Two different liquid-level control scenarios are considered in this comparison and the obtained results show the expected performance of the ROF controller guaranteeing the design objectives.

Key Words
"Coupled-Tank, Robust Control, LMIs, Liquid Level Control,Output Feedback"

Corresponding Author: j.s.esmaeili@gmail.com

1. Introduction

Today, the control systems theory plays an undeniable role in many chemical industries' flow, level, and pressure control processes. Whereas the complexity of most of these processes is increasing day by day, the need for new and efficient control methodologies is highlighted. Because of the complexity and nonlinear behavior of these chemical processes, some of the common classical control approaches such as Proportional Integral Derivative controller (PID) and Linear Quadratic Regulator (LQR), are more common for their low costs and ease of implementation, cannot properly handle the objectives of the process control in terms of the robustness and performance as good as possible. Some research studies have worked on these methodologies Jaafar et al. (2014), Saad et al. (2014), Selamat et al. (2015), Engules et al. (2015), and Dutta et al. (2014). To overcome their low efficiency, the design and implementation of robust and high-performance controllers are proposed in the last years such as by Sekban et al. (2020), Xu et al. (2020), and Mahapatro et al. (2018).

The coupled tank system is a well-known benchmark that is used to verify the performance of the controller design in nonlinear systems and is also used to simulate the nonlinear level process controls. The system's nonlinear behavior is concluded from the different scenarios of the interaction between tanks. Some control approaches are presented for level control of the nonlinear coupled tank system. In some research studies, the SMC (Sliding Mode Control) is designed to control the reference tracking of the system on different platforms Aksu and Coban (2019), Başçi et al. (2016), Dutta et al. (2014), Derdiyok and Başçi (2013), Prusty et al. (2016), Nail et al. (2015), Ayten and Dumlu (2021). This methodology has its pros and cons; robustness to uncertainties and disturbances is its advantage and the large chattering in the control signal and slow tracking response as disadvantages. In many case studies, the Neuro-Fuzzy control and the GA (Genetic Algorithm) are presented by Owa et al. (2013), Yilmaz et al. (2021), Başçi and Derdiyok (2016); Arun and Mohan (2017), Souran et al. (2013), Teng et al. (2003). Adaptive learning, fault tolerance characteristics, and more complex learning algorithms with the large response time and the need for high memory requirements are the advantages and disadvantages of these approaches. In another research, Fue et al. (2021) proposed an optimal reference tracking controller for linear coupled systems and applied it to the coupled tank system.

In the above-stated research works, the nonlinear behavior of the system and the incompatibility of the control objectives make it difficult to accede to the main objectives of the design procedure such as robustness and better reference tracking. Therefore, most of them try to reach a better tradeoff between these incompatible objectives sometimes with trial and error. Hence, according to some weaknesses of the aforementioned methods in dealing with the system's nonlinearity, the H_∞-based feedback control methodology is proposed to satisfy the design objectives of this study. On the other hand, the H_∞-norm is explained as the output's worst-case RMS (Root Mean Square) value. So, the characteristics of the H_∞ synthesis in response to the deterministic inputs and its acceptable performance and robustness in disturbance rejection make it an effective choice for the level control of the system. Generally, the coupled tank system with two main configurations named configurations 1 and 2 is considered in most controller design studies as a case study to verify the effectiveness of their designed controller. Two scenarios cover these configurations: #1 controlling the upper tank liquid level and #2 controlling the bottom tank liquid level in presence of the disturbance of the upper tank output.

This paper is structured as follows; section 2 contains coupled tank system description and its mathematical model. In section 3 the design objectives are explained and the ROF H_∞ control methodology is described mathematically in LMIs. To illustrate the performance of the designed controller the simulations and experimental results have been discussed in section 4. In this section to demonstrate the efficacy of the proposed controller, it is compared to the PI+Feedforward controller experimentally. Comparison between these two controllers is done by computing the Mean Absolute Deviation (MAD) of the reference tracking responses. The last section, section 5, includes the conclusions of the study.

2. Coupled Tank System Description

Two scenarios of configuration #1 and configuration #2, which are described based on the choice of the level control of the tanks, are illustrated in Fig. 1 and Fig. 2. The mathematical descriptions of these configurations are presented in the following.

2.1. First-tank System with Configuration #1

The single-tank system consists of the top tank of the coupled-tank system shown in Fig. 1. The input of the system is the pump flow into the first tank and the bottom tank is not considered. So the voltage of the pump is introduced as the input and the liquid level in the top tank is described as the output of the process.

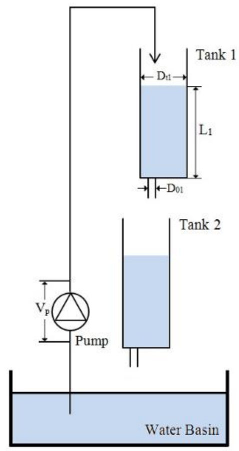

Figure 1. Coupled-tank system schematic diagram: configuration #1

In the stationary consideration of the system, the input liquid flow to the tank is in the same amount as the output flow drained from the system. The difference between these two amounts is accumulated in the tank in the dynamic consideration. Therefore, the mathematical model of configuration #1 is determined by the following equations (Esmaeili and Başçi (2019)):

$$f_{i1} = K_m V_p \quad (1)$$
$$f_{o1} = A_{o1} v_{o1} \quad (2)$$

where K_m is the pump volumetric constant, V_p is the pump input voltage, A_{o1} is the cross-sectional area of the system, and v_{o1} is the outflow velocity of the tank 1. As a remark, the A_{o1} is calculated by,

$$A_{o1} = \frac{1}{4}\pi D_{o1}^2 \quad (3)$$

where D_{o1} denotes the tank 1 outlet diameter. Bernoulli's equation can calculate the outflow velocity

$$v_{o1} = \sqrt{2gL_1} \quad (4)$$

where g and L_1 are the gravitational constant($\cong 981\, cm/sec^2$) and the height of the fluid in tank1, respectively. Substituting the presented equations into equation (2), the outflow rate of tank 1 becomes,

$$f_{o1} = A_{o1}\sqrt{2gL_1} \quad (5)$$

As mentioned before, the difference between the input and output flow is accumulated in the tank and this difference can be written as a mass balance principle by the following first-order differential equation

$$A_{t1}\left(\frac{\partial}{\partial t}L_1\right) = f_{i1} - f_{o1} \quad (6)$$

where A_{t1} is the inside cross-sectional area of tank 1. Rewriting the equation (6) with eqs. (1) and (2) can be denoted in the following form:

$$\frac{\partial}{\partial t}L_1 = -\frac{A_{o1}}{A_{t1}}\sqrt{2gL_1} + \frac{K_m}{A_{t1}}V_p \quad (7)$$

2.2. Coupled Tank System as Configuration #2

Fig. 2 illustrates configuration #2 of the coupled-tank plant. According to the schematic diagram of the second configuration, tank 1 is fed by the pump, and the outlet of tank 1 is fed into tank 2. The liquid level of tank 1 and tank 2 are the states of the system in this configuration. The state-space equation for tank 1 is the same one in equation (7). For the bottom tank 2, the outlet flow rate can be described as

$$f_{o2} = A_{o2} v_{o2} \quad (8)$$

The tank 2 outflow velocity using Bernoulli's formula is

$$v_{o2} = \sqrt{2gL_2} \tag{9}$$

In the same form as in the previous configuration, the cross-sectional area of the outlet of tank 2 is calculated by

$$A_{o2} = \frac{1}{4}\pi D_{o2}^2 \tag{10}$$

The outlet flow rate of tank 1 is considered as the input flow to tank 2. So using Eq. (5) the input flow of tank 2 is

$$f_{i2} = f_{o1} = A_{o1}\sqrt{2gL_1} \tag{11}$$

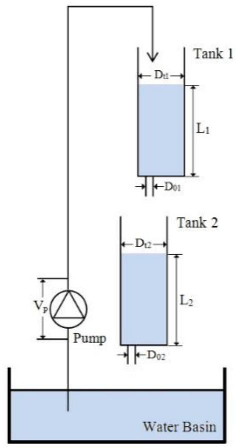

Figure 2. Coupled-tank system schematic diagram: configuration #2

Considering the mass balance rule for tank 2, the differential equation for tank 2 is obtained as follows

$$A_{t2}\left(\frac{\partial}{\partial t}L_2\right) = f_{i2} - f_{o2} \tag{12}$$

Substituting Eqs. (8) and (11) into equation (12) give the state-space realization for the level of tank 2 as follows:

$$\frac{\partial}{\partial t}L_2 = \frac{A_{o1}}{A_{t2}}\sqrt{2gL_1} - \frac{A_{o2}}{A_{t2}}\sqrt{2gL_2} \tag{13}$$

Eqs. (7) and (13) are considered as main equations of the coupled-tank system, and the state variables will be as below

$$x_1(t) = L_1$$
$$x_2(t) = L_2$$

Using the linearization principle around the equilibrium point of the system as (L_{01}, L_{02}), the state-space representation of the LTI (Linear Time Invariant) system is described by:

$$\dot{x}(t) = Ax(t) + Bu(t)$$

with

$$A = \begin{bmatrix} -\frac{A_{o1}}{A_{t1}}\sqrt{\frac{g}{2L_{01}}} & 0 \\ \frac{A_{o1}}{A_{t2}}\sqrt{\frac{g}{2L_{01}}} & -\frac{A_{o2}}{A_{t2}}\sqrt{\frac{g}{2L_{02}}} \end{bmatrix},\ B = \begin{bmatrix} \frac{K_m}{A_{t1}} \\ 0 \end{bmatrix} \tag{14}$$

3. LMI-Based ROF Synthesis Description

3.1. H_∞ Norm

There are several descriptions for the H_∞ norm in the time and frequency domains. In generality, the main goal of designing this controller is to minimize the H_∞ norm of the system's transfer function. In the frequency domain representation, the H_∞ norm minimizes the biggest singular value of the system, and in the SISO case; it is the largest input/output RMS gain of the transfer function. The H_∞ norm is described as the following:

$$\|G(s)\|_\infty \triangleq \sup_{\omega} \bar{\sigma}(G(j\omega)) \tag{15}$$

The time-domain expression of the H_∞ norm is named the induced 2-norm as follows (Esmaeili et al. 2015):

$$\|G(s)\|_\infty = \sup_{w(t)\neq 0} \frac{\|z(t)\|_2}{\|w(t)\|_2} \tag{16}$$

where $\|z(t)\|_2 = \sqrt{\int_0^\infty \sum_i |z_i(t)|^2\, dt}$ is the energy of the signal vector. It minimizes the energy of the output signal for the worst-case input signal Esmaeili et al. (2015).

3.2. Design Objectives

As mentioned before, in this study the main aims of the controller design are the reference setpoint tracking by considering the structural constraints of the nonlinear system. On the other hand, some unexpected inputs such as disturbances and sensor noise which the system must be isolated from are considered uncertainties in the design procedure. So these objectives, which are to be taken into consideration in designing the controller, are listed as follows:

- Minimization of the reference tracking error: to have better reference tracking in the level control, it has to be minimized the setpoint liquid level tracking error. Fast accurate reference tracking with minimum error has an important role in process control applications.

- Disturbance rejection: Besides the main input of the system named as the reference setpoint, sometimes there are other types of unexpected exogenous inputs such as disturbances and sensor noises. The need for a robust controller is highlighted to isolate the system from and overcome these unwelcome inputs. This objective of designing a procedure motivates the disturbance rejection characteristic of the H_∞ controller.

- Control signal: the upper and lower bounds of the water pump input voltage are considered the structural constraints of the system, so the control signal constraint is determined as below:

$$|u| \leq u_{max}$$

3.3. Robust Output Feedback Synthesis

The design framework of the augmented plant is shown in Fig. 3. To negate the frequency effects of the exogenous inputs of the system, it is undeniable to add some weights on the system inputs [L_{ref} n_1 n_2] and desired control outputs [Z_e Z_u]. In other words, the input and output weights explain the frequency content of the inputs and the interested frequencies of controlled outputs (Esmaeili et al. (2015)). The [y_1 y_2] are measured using sensors which are described as the measured outputs of the tank levels.

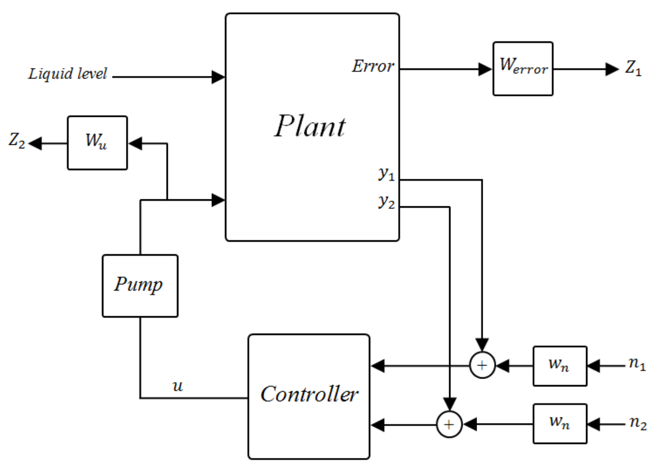

Figure 3. Augmented Plant model

Now the state-space realization of the augmented plant for designing the H_∞ control is described below:

$$\dot{x}(t) = Ax(t) + B_1\omega(t) + B_2u(t) \tag{17. a}$$
$$z(t) = C_1x(t) + D_{11}\omega(t) + D_{12}u(t) \tag{17. b}$$
$$y(t) = C_2x(t) + D_{21}\omega(t) + D_{22}u(t) \tag{17. c}$$

To design the H_∞ controller the controller is described as

$$S := \begin{pmatrix} \dot{x}_c \\ u \end{pmatrix} = \begin{pmatrix} A_c & B_c \\ C_c & D_c \end{pmatrix} \begin{pmatrix} x_c \\ y \end{pmatrix} \tag{18}$$

and the closed-loop system realization is described as

$$\begin{gathered} \mathcal{A}_{cl} := \begin{pmatrix} A + B_2D_cC_2 & B_2C_c \\ B_cC_2 & A_c \end{pmatrix} \\ \mathcal{B}_{cl} := \begin{pmatrix} B_1 + B_2D_cD_{21} \\ B_cD_{21} \end{pmatrix} \\ \mathcal{C}_{cl} := (C_1 + D_{12}D_cC_2 \quad D_{12}C_c) \\ \mathcal{D}_{cl} := D_{11} + D_{12}D_cD_{21} \end{gathered} \tag{19}$$

Considering the linear dissipative systems theory that Gahinet et al. (1994) have presented, the following BMI (Bilinear Matrix Inequality) gives the controller:

Minimize γ_∞ subject to

$$K \succ 0 \tag{20}$$

$$\begin{pmatrix} \mathcal{A}_{cl}^T K + K\mathcal{A}_{cl} & K\mathcal{B}_{cl} & \mathcal{C}_{cl}^T \\ * & -\gamma_\infty^2 I & \mathcal{D}_{cl}^T \\ * & * & -I \end{pmatrix} \prec 0$$

As the inequality described in (20) involves nonlinear terms, this BMI (Bilinear Matrix Inequality) must be changed to an LMI using a change of variables and the proper congruence transformation (Gahinet et al. (1994), Scherer and Weiland (2000)). So these new variables are described as follows:

$$\left(K, \begin{pmatrix} A_c & B_c \\ C_c & D_c \end{pmatrix}\right) \rightarrow \ v = \left(\boldsymbol{X}, \ \boldsymbol{Y}, \ \begin{pmatrix} \widetilde{\boldsymbol{A}} & \widetilde{\boldsymbol{B}} \\ \widetilde{\boldsymbol{C}} & \widetilde{\boldsymbol{D}} \end{pmatrix}\right) \tag{21}$$

The matrix K is chosen in such a way that

$$K = \begin{pmatrix} \boldsymbol{X} & M \\ M^T & * \end{pmatrix}, \ K^{-1} = \begin{pmatrix} \boldsymbol{Y} & N \\ N^T & * \end{pmatrix} \tag{22}$$

that the matrices X and Y are symmetric and in the same dimension as the matrix A which are satisfied $MN^T = I - \boldsymbol{XY}$.

$$\mathcal{Y} = \begin{pmatrix} \boldsymbol{Y} & I \\ N^T & 0 \end{pmatrix} \tag{23}$$
$$\mathcal{Y}^T K \mathcal{Y} = \begin{pmatrix} \boldsymbol{Y} & I \\ I & \boldsymbol{X} \end{pmatrix} \tag{24}$$
$$\mathcal{Y}^T (K\mathcal{A}) \mathcal{Y} := \begin{pmatrix} A\boldsymbol{Y} + B_2\widetilde{\boldsymbol{C}} & A + B_2\widetilde{\boldsymbol{D}}C_2 \\ \widetilde{\boldsymbol{A}} & \boldsymbol{X}A + \widetilde{\boldsymbol{B}}\boldsymbol{C_2} \end{pmatrix} \tag{25}$$
$$\mathcal{Y}^T (K\mathcal{B}) := \begin{pmatrix} B_1 + B_2\widetilde{\boldsymbol{D}}D_{21} \\ \boldsymbol{X}B_1 + \widetilde{\boldsymbol{B}}D_{21} \end{pmatrix} \tag{26}$$
$$\mathcal{Y}^T \mathcal{C} := (C_1\boldsymbol{Y} + D_{12}\widetilde{\boldsymbol{C}} \quad C_1 + D_{12}\widetilde{\boldsymbol{D}}C_2) \tag{27}$$

Choosing the abovementioned transformations, the LMI of the ROF controller is obtained as follows:

$$\begin{pmatrix} \boldsymbol{X} & I_n \\ I_n & \boldsymbol{Y} \end{pmatrix} > 0, \tag{28}$$

$$\begin{pmatrix} A\boldsymbol{X} + \boldsymbol{X}A^T + B_2\widetilde{\boldsymbol{C}} + \widetilde{\boldsymbol{C}}^T B_2^T & * & * & * \\ \tilde{A} + A^T + C_2^T \widetilde{\boldsymbol{D}}^T B_2^T & \boldsymbol{Y}A + A^T\boldsymbol{Y} + \widetilde{\boldsymbol{B}}C_2 + C_2^T\widetilde{\boldsymbol{B}}^T & * & * \\ B_1^T + D_{21}^T\widetilde{\boldsymbol{D}}^T B_2^T & B_1^T\boldsymbol{Y} + D_{21}^T\widetilde{\boldsymbol{B}}^T & -\gamma_\infty I_{n_u} & * \\ C_1\boldsymbol{X} + D_{12}\widetilde{\boldsymbol{C}} & C_1 + D_{12}\widetilde{\boldsymbol{D}}C_2 & D_{11} + D_{12}\widetilde{\boldsymbol{D}}D_{21} & -\gamma_\infty I_{n_y} \end{pmatrix} < 0$$

The unknown parameters $\widetilde{\boldsymbol{D}}, \widetilde{\boldsymbol{C}}, \widetilde{\boldsymbol{B}}, \widetilde{\boldsymbol{A}}, \boldsymbol{Y}, \boldsymbol{X}$ obtain from solving the above LMIs. Finally, the controller parameters are given by using the following (Gahinet et al. (1994)):

$$\begin{cases} \widetilde{\boldsymbol{D}} = D_c \\ \widetilde{\boldsymbol{C}} = D_cC_2X + C_cM^T \\ \widetilde{\boldsymbol{B}} = YB_2D_c + NB_c \\ \widetilde{\boldsymbol{A}} = YAX + YB_2D_cC_2X + NB_cC_2X + YB_2C_cM^T + NA_cM^T \end{cases} \tag{29}$$

where M and N are square and nonsingular matrices with $MN^T = I - \boldsymbol{XY}$. From Eq. (29) the controller matrices are obtained as below:

$$\begin{cases} D_c = \widetilde{\boldsymbol{D}} \\ C_c = \left(\widetilde{\boldsymbol{C}} - D_cC_2X\right) * (M^T)^{-1} \\ B_c = (N)^{-1} * \left(\widetilde{\boldsymbol{B}} - YB_2D_c\right) \\ A_c = (N)^{-1} * \left(\widetilde{\boldsymbol{A}} - YAX - YB_2D_cC_2X - NB_cC_2X - YB_2C_cM^T\right) * (M^T)^{-1} \end{cases} \tag{30}$$

4. PI+Feedforward Controller Design

Proportional-Integral controllers are one of the most employed controllers in a wide range of industrial processes due to their relative simplicity and low cost of implementation. The great success of these controllers is due to the implementation of their additional functionalities such as feedforward action (Veronesi and Visioli (2013)). Although the PI controller minimizes small changes and oscillations of the output from its operating point, the feedforward control can promote the disturbance rejection performance of the controller and reference tracking of the system. The block diagram of the PI+ feedforward controller is demonstrated in Fig. 4. Because the plant doesn't involve an integrator, the parameters of the controller are adjusted from the first method of the Ziegler-Nicoles methodology as follows (Åström and Hägglund (2004), Ziegler and Nichols (1942))

$$C_{PI}(s) = K_p\left(1 + \frac{1}{T_i s}\right) \tag{31}$$

$$K_p = 0.45K_{cr}\,, \qquad T_i = \frac{1}{1.2}P_{cr}$$

which K_{cr} and P_{cr} represent the critical gain and period, respectively.

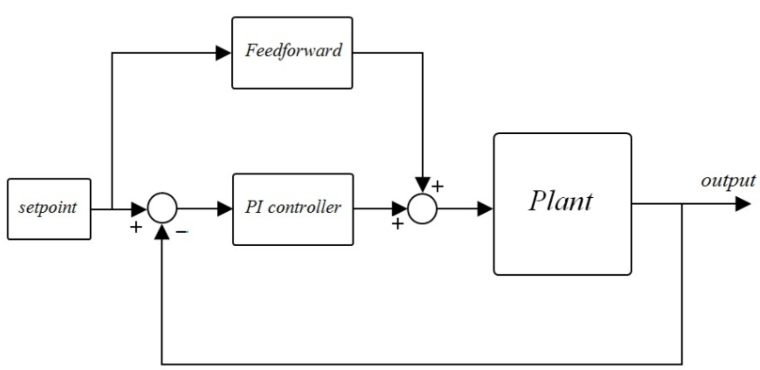

Figure 4. Block diagram of closed-loop PI Feedforward system

5. Experimental Results

After designing the ROF controller in the previous section, the simulation and experimental results of the closed-loop coupled tank system with two configurations 1 and 2 are expressed in this section. The performance of the designed controller is tested on the real coupled tank system setup. Fig. 5 shows this setup of the Quanser coupled tank system. The results are compared with the PI+feedforward controller to demonstrate the effectiveness and superiority of the ROF H∞ controller methodology and improvements to the design objectives. To have a good view of the performance comparison of these controllers, the Mean Absolute Deviation (MAD) methodology is used. In this mathematical method, the difference between the reference signal and the experimental data is calculated as $y - \hat{y}$ that the reference liquid level of the tank is denoted as y, and $\hat{y}$ is the experimental tracking level. This residual can be positive or negative as the tracking level moves above or under the reference level signal. So, averaging the absolute value of the error $(y - \hat{y})$ calculates the MAD as the below equation:

$$MAD = \frac{1}{n}\sum_{i=1}^{n}|y_i - \hat{y}_i| \tag{32}$$

which n is the sample number.

Figure 5. Quanser Coupled tank system setup

5.1. Configuration #1

According to the augmented plant model of the system mentioned in the third section, to satisfy the design frequency response requirements in reference tracking and noise rejection some weights need to be added to the exogenous inputs and controlled outputs. These weights are introduced as follows:

$$W_n = 0.001$$
$$W_{error} = \frac{s + 3.1}{s^2 + 26s + 85}$$
$$W_u = 0.0001$$

which the W_n represents the weight on the noise input and W_{error} is chosen as the weight on the closed-loop error wishing for good reference tracking. In configuration 1 choosing the first order of the W_n increases the order of the designed controller, so it is chosen as a constant gain that reduces the possible effect of the noise on the system's sensor. The W_u has to be chosen as a small constant near zero to dispel the singularity in the controller at high frequencies, and W_{error} is chosen based on the frequency characteristics of the desired level tracking signal. Interested readers in choosing the weights on the control objectives are referred to for more details (Skogestad and Postlethwaite (2007); Zhou et al. (1996)). Fig. 6a and Fig. 6b illustrate the comparison of the simulation and experimental results of the ROF H_∞ vs. PI+feedforward. In this configuration, the reference level is set to 10 cm adding different sinusoidal and square signals to show the efficiency of the ROF approach. The parameters of the coupled-tank system are introduced in Table 1.

Table 1. Parameter Values of the Coupled-tank System

Description	Symbol	Value	Units
Cross sections area of Tanks	$A_1 = A_2$	15.5179	cm^2
Outflow orifices areas of Tanks	$a_1 = a_2$	0.1781	cm^2
Pump volumetric constant	K_m	4.6	$(cm^3/sec)/V$

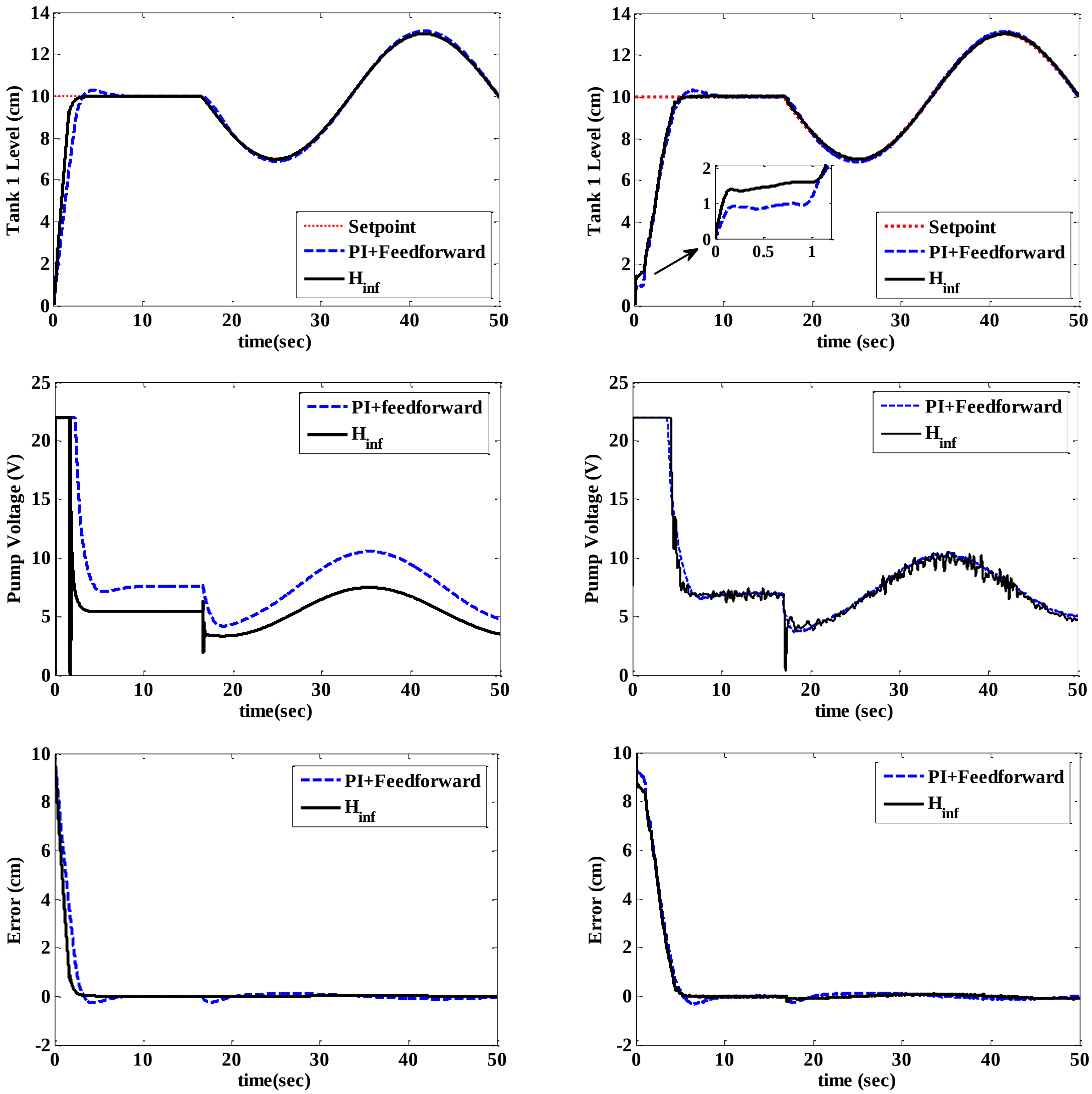

(a) (b)

Figure 6. Comparison of ROF H_∞ and PI feedforward controllers on configuration 1; constant with sinusoidal reference: a) simulation results; b) experimental results.

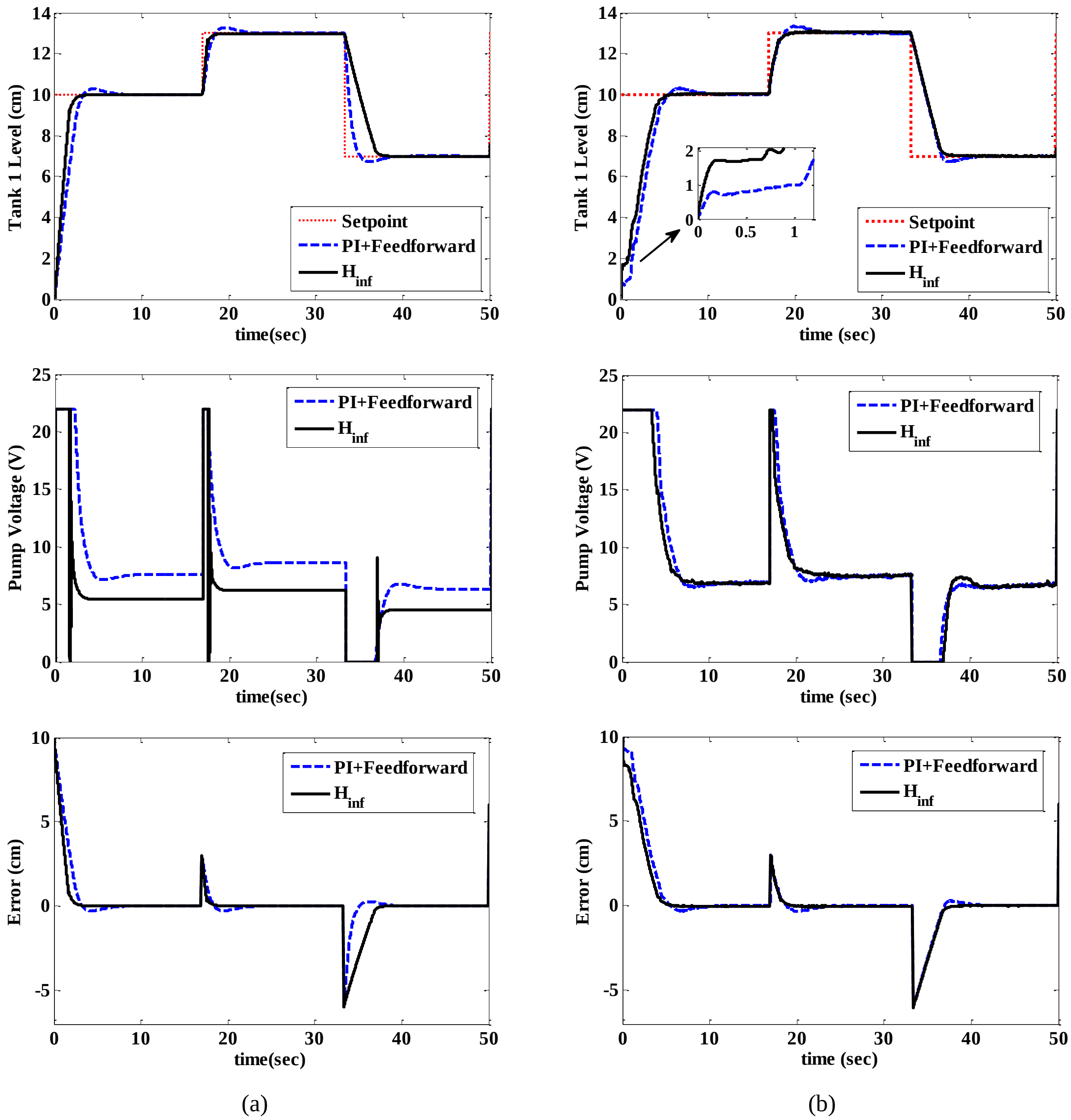

Figure 7. Comparison of ROF H_∞ and PI feedforward controllers on configuration #1; constant with square setpoint: a) simulation results; b) experimental results.

According to Fig. 6 and Fig. 7, the ROF H_∞ controller has a considerable performance improvement in the reference setpoint track versus the PI feedforward. The MAD values of the two controllers are shown in Tables 2 and 3 to mathematically evaluate these controllers' performance.

Table 2. Mean Absolute Deviation values on Sinusoidal Reference Setpoint

Controller	Constant part	Sinusoidal part	Total MAD
PI+ feedforward	1.4637	0.0834	0.5528
ROF H_∞	1.2661	0.0589	0.4694

Table 3. Mean Absolute Deviation values on Square Reference Setpoint

Controller	Constant part	Square part	Total MAD
PI+ feedforward	1.5413	0.4310	0.8085
ROF H_∞	1.2025	0.4127	0.6813

According to tables 2 and 3, the ROF H_∞ controller versus the PI+ feedforward has considerable improvement in setpoint tracking of the sinusoidal and square inputs about 15% and 15.7%, respectively.

5.2. Configuration #2

In this scenario, the main goal is to set the liquid level of the second tank at the setpoint level besides the satisfaction of the system's robustness in the existence of the output noises and disturbance. Similar to the previous section, according to the design objectives similar to the previous design, some weights are added to the system. These weights are described below:

$$W_n = \frac{7}{s + 0.31}$$
$$W_{error} = \frac{100}{s + 85}$$
$$W_u = 0.0001$$

Considering the previous section descriptions, these weights are chosen based on the augmented system's frequency needs and the system's sensitivity function and need some trial and error methods. After solving the related LMIs of ROF H_∞ controller synthesis, the obtained controller has a high order of four. This controller adds extra states to the system which causes difficulties such as low response time. Hence, using the order reduction function in MATLAB the order of the controller is reduced to two by eliminating unnecessary Hankel singular values. This order reduction and the related frequency responses of the controller transfer function and its reduced order are shown in Fig. 8.

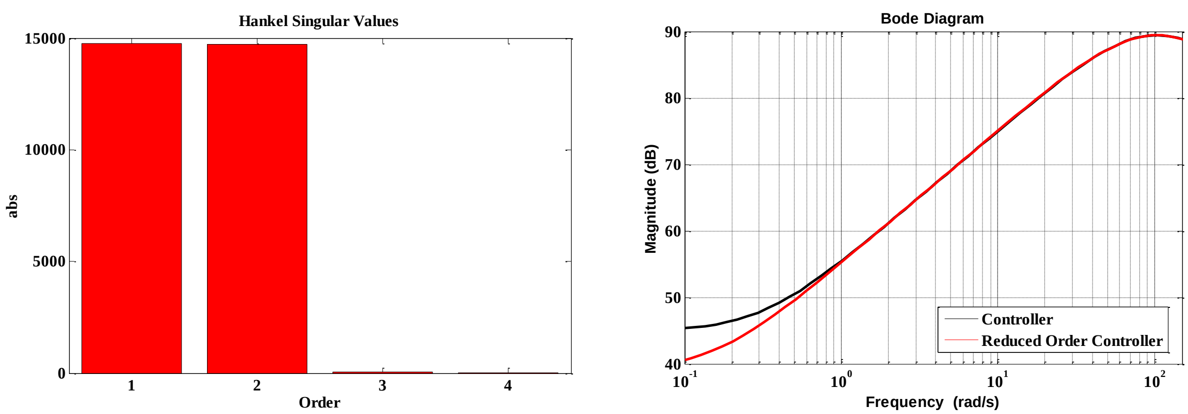

Figure 8. ROF H_∞ Controller Order Reduction (Hankel Singular Values)

Fig. 9 contains the results comparison of the nonlinear system using two controllers. As shown in Fig. 9, the proposed ROF controller has perfect setpoint tracking in tank 2 and its performance improvement against the PI+feedforward controller is about a total of 27.8%. The mathematical comparison of two controllers using the mean absolute deviation of tracking errors is obtained in table 4.

Table 4. Mean Absolute Deviation values on Sinusoidal Reference Setpoint

Controller	Constant part	Sinusoidal part	Total MAD
PI+ feedforward	2.3516	0.3430	0.8452
ROF H_∞	2.1300	0.1039	0.6104

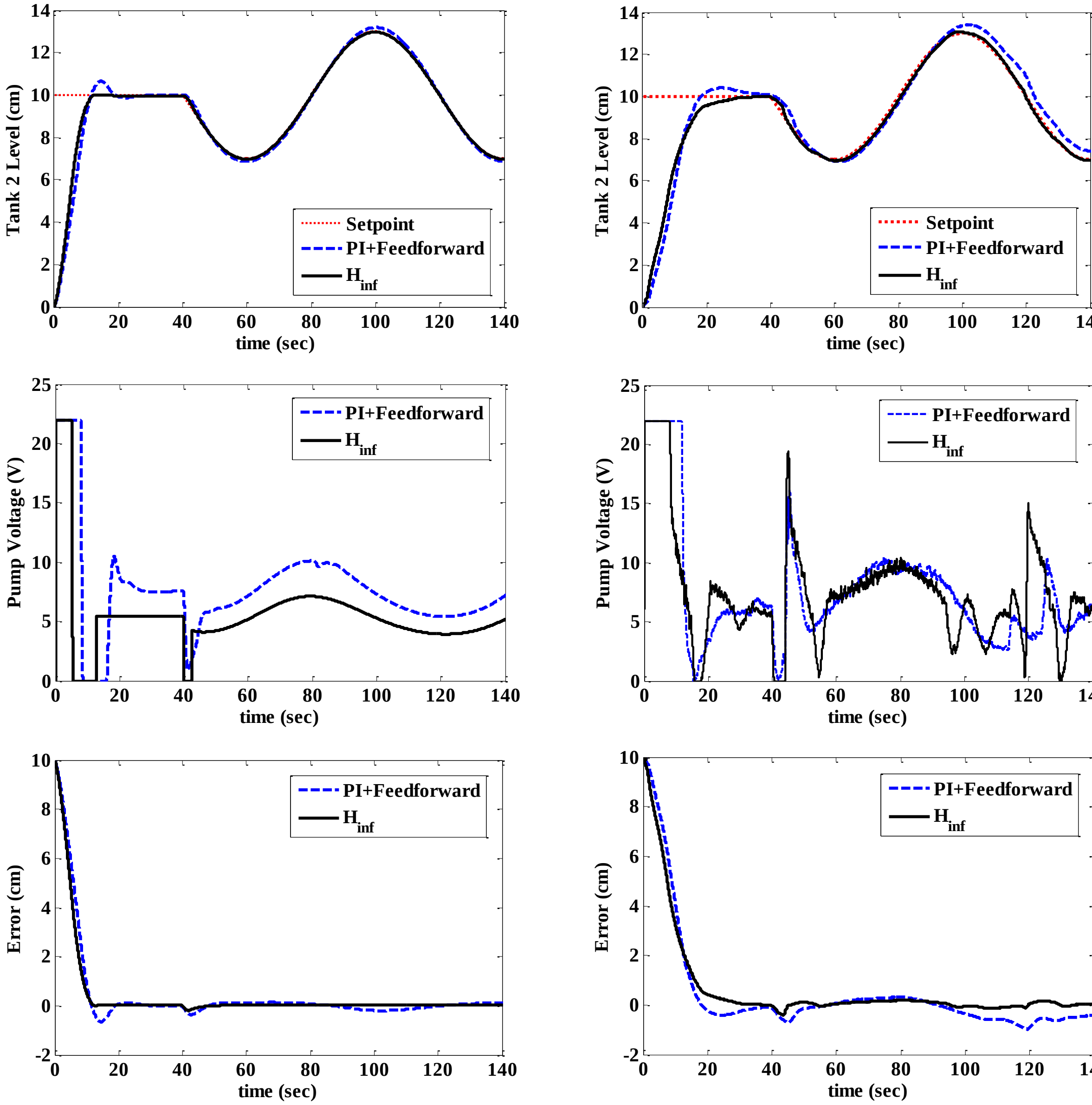

(a) (b)

Figure 9. Comparison of ROF H_∞ and PI+feedforward controllers on configuration 2; constant with sinusoidal setpoint: a) simulation results; b) experimental results.

6. Conclusion

In this experimental study, a ROF H_∞-based controller is proposed to use in the control of the liquid level in a vertical coupled tank system as a case study system in the simulation of large-scale process controls. The verification of the designed controller is done in a procedure consisting of two configuration scenarios named configuration #1 and #2, in which the main goal is the setpoint level tracking in tanks 1 and 2, respectively, besides satisfying the design objectives, as the robustness of the system by reducing the effects of the disturbance and sensor noises besides the good setpoint tracking and a tradeoff between structural constraints. The synthesis of the proposed approach is done using LMIs to handle the existence of the estimated singularities in the system and adjust the design objectives simultaneously. Whereas in the second tank control the designed controller has a high order, the order reduction methodology is used to decrease the order of the controller with retaining the frequency characteristics of the main one. The good performance of the proposed robust controller is shown in simulation results in comparison to the PI+feedforward controller and verified with experimental results using both controllers. Attained results demonstrate the perfect improvements in the performance of the closed-loop system by about 15% in level control of tank 1 and 28% in reference tracking in tank 2.

Designing a mixed robust controller and comparison to the last designs for the coupled tank system and improvement of the system performance is the future scope of the authors.

References

Aksu, I. O., & Coban, R. (2019). Sliding mode PI control with backstepping approach for MIMO nonlinear cross-coupled tank systems. *International Journal of Robust and Nonlinear Control*, 29(6), 1854-1871.

Arun, N. K., & Mohan, B. M. (2017). Modeling, stability analysis, and computational aspects of some simplest nonlinear fuzzy two-term controllers derived via center of area/gravity defuzzification. *ISA transactions*, *70*, 16-29.

Åström, K. J., & Hägglund, T. (2004). Revisiting the Ziegler–Nichols step response method for PID control. *Journal of process control*, *14*(6), 635-650.

Ayten, K. K., & Dumlu, A. (2021). Implementation of a PID Type Sliding-Mode Controller Design Based on Fractional Order Calculus for Industrial Process System. *Elektronika ir Elektrotechnika*, *27*(6), 4-10.

Başçi, A., & Derdiyok, A. (2016). Implementation of an adaptive fuzzy compensator for coupled tank liquid level control system. *Measurement*, *91*, 12-18.

Başçi, A., Sekban, H. T. & Can, K. (2016). Real-Time Application of Sliding Mode Controller for Coupled Tank Liquid Level System. *International Journal of Applied Mathematics Electronics and Computers*, Special Issue (2016), 301-306.

Derdiyok, A., Başçi, A. (2013). The application of chattering-free sliding mode controller in coupled tank liquid-level control system. *Korean J. Chem. Eng*. 30, 540–545.

Dutta, S., Seal, S., & Sengupta, A. (2014, September). Real-time linear quadratic versus sliding mode liquid level control of a coupled tank system. In *2014 International Conference on Devices, Circuits, and Communications (ICDCCom)* (pp. 1-6). IEEE.

Engules, D., Hot, M., & Alikoc, B. (2015, June). Level control of a coupled-tank system via eigenvalue assignment and LQG control. In *2015 23rd Mediterranean Conference on Control and Automation (MED)* (pp. 1198-1203). IEEE.

Esmaeili, J. S., & Başçi, A. (2019, July). LMI-based H_2 Control of Vertical Nonlinear Coupled-tank System. In *2019 International Conference on Control, Automation and Diagnosis (ICCAD)* (pp. 1-7). IEEE.

Esmaeili, J. S., Akbari, A., & Karimi, H. R. (2015). Load-dependent LPV/H2 output-feedback control of semi-active suspension systems equipped with MR damper. *International Journal of Vehicle Design*, *68*(1-3), 119-140.

Fu, Y., Chen, W., & Fu, J. (2021). A New Optimal Tracking Controller of Linear Strongly Coupled Systems and Its Applications. *IEEE Transactions on Circuits and Systems II: Express Briefs*, *69*(3), 1387-1391.

Gahinet, P., Nemirovskii, A., Laub, A. J., & Chilali, M. (1994, December). The LMI control toolbox. In *Proceedings of 1994 33rd IEEE Conference on Decision and Control* (Vol. 3, pp. 2038-2041). IEEE.

Jaafar, H. I., Hussien, S. Y. S., Selamat, N. A., Aras, M. S. M., & Rashid, M. Z. A. (2014). Development of PID controller for controlling the desired level of coupled tank system. *International Journal of Innovative Technology and Exploring Engineering*, *3*(9), 32-36.

Khalil, I. S., Doyle, J. C., & Glover, K. (1996). *Robust and optimal control*. Prentice-Hall.

Mahapatro, S. R., Subudhi, B., & Ghosh, S. (2019). Design and experimental realization of a robust decentralized PI controller for a coupled tank system. *ISA transactions*, 89, 158-168.

Nail, B., Bekhiti, B., Bdirina, K., Kouzou, A., & Hafaifa, A. (2015, May). Sliding mode control and optimal GPC algorithm for coupled tanks. In *2015 3rd International Conference on Control, Engineering & Information Technology (CEIT)* (pp. 1-6). IEEE.

Owa, K. O., Sharma, S. K., & Sutton, R. (2013). Optimized multivariable nonlinear predictive control for coupled tank applications.

Prusty, S. B., Seshagiri, S., Pati, U. C., & Mahapatra, K. K. (2016, January). Sliding mode control of coupled tanks using conditional integrators. In *2016 Indian Control Conference (ICC)* (pp. 146-151). IEEE.

Quanser manufacturer, https://www.quanser.com

Saad, M., Albagul, A., & Abueejela, Y. (2014). Performance comparison between PI and MRAC for coupled-tank system. *Journal of Automation and Control Engineering Vol*, *2*(3).

Scherer, C., & Weiland, S. (2000). Linear matrix inequalities in control. *Lecture Notes, Dutch Institute for Systems and Control, Delft, The Netherlands*, *3*(2).

Sekban, H. T., Can, K., Basci, A. (2020). Model-based Dynamic Fractional-order Sliding Mode Controller Design for Performance Analysis and Control of a Coupled Tank Liquid-level System, *Advances in Electrical and Computer Engineering*, vol.20, no.3, pp.93-100.

Selamat, N. A., Daud, F. S., Jaafar, H. I., & Shamsudin, N. H. (2015, March). Comparison of LQR and PID controller tuning using PSO for Coupled Tank System. In *2015 IEEE 11th International Colloquium on Signal Processing & Its Applications (CSPA)* (pp. 46-51). IEEE.

Skogestad, S., & Postlethwaite, I. (2007). *Multivariable feedback control: analysis and design* (Vol. 2). New York: Wiley.

Souran, D. M., Abbasi, S. H., & Shabaninia, F. (2013). Comparative study between tank's water level control using PID and fuzzy logic controller. In *Soft computing applications* (pp. 141-153). Springer, Berlin, Heidelberg.

Teng, T. K., Shieh, J. S., & Chen, C. S. (2003). Genetic algorithms applied in online autotuning PID parameters of a liquid-level control system. *Transactions of the Institute of Measurement and Control*, *25*(5), 433-450.

Veronesi, M., & Visioli, A. (2013, July). Automatic feedforward tuning for PID control loops. In *2013 European Control Conference (ECC)* (pp. 3919-3924). IEEE.

Xu, T., Yu, H., Yu, J., & Meng, X. (2020). Adaptive disturbance attenuation control of two tank liquid level system with uncertain parameters based on port-controlled Hamiltonian. *IEEE Access*, 8, 47384-47392.

Yılmaz, M. , Can, K. & Başçi, A. (2021). PI+Feed Forward Controller Tuning Based on Genetic Algorithm for Liquid Level Control of Coupled-Tank System. *Journal of the Institute of Science and Technology*, 11 (2), 1014-1026.

Ziegler, J. G., & Nichols, N. B. (1942). Optimum settings for automatic controllers. *trans. ASME*, *64*(11).